Effect of crystal field on the magnetization of dilute hcp alloys

L. A. Moberly,* R. Roshko, and O. G. Symko
Department of Physics, University of Utah, Salt Lake City, Utah 84112
(Received 20 October 1981)

Magnetization measurements on very dilute single-crystal alloys of Mg-Mn, Zn-Mn, and Zn-Cr in the temperature range of 2–0.008 K show that the ground state of these systems is determined by fine-structure splitting. For Mg-Mn the fine-structure constant D is +0.006 K with an effective spin of $\frac{5}{2}$ while for Zn-Mn D is −0.07 K and for Zn-Cr it is +0.08 K for an effective spin of 1 in both cases. Over our temperature range there is no evidence for a Kondo spin-compensated state. For all impurity concentrations, even the 1 ppm level, Ruderman-Kittel-Kasuya-Yosida interactions play an important role as determined from magnetization measurements of polycrystalline Zn-Mn alloys.

I. INTRODUCTION

This study deals with the low-temperature single-impurity behavior of Mn and Cr impurities in hcp metallic hosts such as Zn and Mg. Although these systems have been studied extensively[1–4] the nature of the single impurity ground state has never been established because the temperature range was not low enough and quite often impurity-impurity interactions masked the true single impurity state. The impurity-impurity effects caused by the Ruderman-Kittel-Kasuya-Yosida (RKKY) interaction between the impurities are by themselves interesting and have led to a wide range of interesting effects known as spin-glass behavior.[5,6] In order to assess the importance of the impurity-impurity interactions, which vary with concentrations, we have investigated the magnetization of polycrystalline Zn-Mn alloys in the temperature range of 8 mK to 2 K for Mn concentrations ranging from 1 to 65 ppm. The results show that indeed magnetic impurity concentrations in these alloys have to be of order of 1 ppm or less for single impurity effects to be seen.

The nature of the single impurity ground state is complex because of the various possibilities that can exist. Usually most of the dilute magnetic alloys have been characterized at low temperatures by a Kondo spin-compensated state.[1,4] Such a state arises from a compensation of the local impurity moment by the conduction electrons as a result of an antiferromagnetic exchange coupling between the impurity and the conduction electrons. The temperature at which spin compensation is expected to take place is known as the Kondo temperature T_K. For Zn-Mn, T_K is claimed to be ~ 0.45 K while for Zn-Cr it is 0.48 K. Such Kondo temperatures are usually obtained from high-temperature Curie-Weiss behavior,[1,4] the Curie-Weiss temperature being of order T_K. This, of course, assumes that all other contributions to the Curie-Weiss temperature can be neglected. Even then, for a given system there is quite a variation on the reported T_K depending on the group that measured it, on the sample (for example, Ref. 1 claims that T_K for Zn-Mn is 0.25 K while Ref. 7 claims it to be 0.9 K) and on the method used to measure it. It is our belief that the true nature of the Kondo spin-compensated state has not been established clearly as high-temperature data can only give a Curie-Weiss temperature which gives some insight into the ordered state. Hence, this study is aimed at investigating at very low temperatures the Kondo state for Mn and Cr impurities in hcp hosts, Zn and Mg, and any other single impurity interaction that may exist in these systems.

Single impurity effects other than the Kondo effect which have to be taken into account, but which usually have been ignored, are crystal fields and hyperfine interactions. Actually, high-temperature susceptibility studies[1] on single crystals of Zn-Mn and Zn-Cr have been analyzed in terms of a Kondo effect with $T_K = 0.25$ K and a crystal field whose fine structure splitting parameter $D = -78$ mK for Mn impurities and $D = +84$ mK for Cr impurities. These effects were extracted from the measured Curie-Weiss temperature. However, in these measurements impurity-impurity interactions were entirely ignored even though the impurity concentrations were relatively high.

In order to investigate the above single impurity effects, we first studied S-state impurity ions, Mn^{2+}, in Zn single crystals. Cr impurities, which are non-S state, were investigated in the same host Zn, also in single crystal samples. Manganese impurities were investigated first since they have only spin angular momentum and hence are expected to be simpler to analyze, while Cr impurities introduce an additional complication due to the possibility of a contribution from the finite orbital angular momentum. Because

magnetic impurities in the Zn host have strong exchange interactions with the conduction band (the free ion spin of Mn^{2+} is modified from $S=\frac{5}{2}$ to an effective spin of $S=1$ in Zn), we also studied a system where the effects of exchange are weaker and where the ionic approach to the magnetic impurity problem would be more applicable. This led us to investigate the magnetization of Mn in single crystals of Mg (here the effective spin is $\approx\frac{5}{2}$, being close to its ionic value). The hosts Zn and Mg have an hcp structure, and consequently any crystal field acting on the impurity will possess axial symmetry. Due to this symmetry, the magnetization was expected to be anistropic and hence measurements were performed along the two principal axes of the crystal: the c axis and the a axis.

Finally, in analyzing our data, we have also considered the possibility of hyperfine interactions since in our low-temperature regime these interactions can be important.

Section II of the paper deals with the experimental procedure and the method used for making samples at the 1-ppm level. The results and their analysis are presented in Sec. III. The discussion Sec. IV deals with the explanation of the results in terms of fine structure, the importance of hyperfine interactions, and the absence of a Kondo spin-compensated state in our temperature range.

II. EXPERIMENTAL DETAILS

The polycrystalline Zn-Mn samples were prepared in an induction furnace from 99.9999% purity Zn and 99.99% purity Mn. The samples were quenched from the melt. They were machined and etched to a cylinder of size 6.0 mm length by 2.8 mm diameter.

The single crystal Zn-Mn and Zn-Cr samples were grown by the unseeded Bridgman technique. The Zn host was prepurified by melting under hydrogen. Usually the single crystals were 10 to 30 times the size of the final sample. For the magnesium alloys, magnesium of initial purity 99.999% was distilled until the Mn, Fe, and Cr impurity levels were below 1 ppm as determined by a spectroscopic test analysis. Here as well, single crystals were grown by the Bridgman technique. After x-ray orienting, cylindrical samples were spark cut along the c axis and along the a axis, next to each other in the bulk sample. All the samples were cut approximately twice the required diameter so that they could be heavily etched to remove any damage at the surface of the crystals. The single crystal samples as used in the experiment were approximately 6 mm long by 2.5 mm diameter.

A sample of the pure host was cut identical in size to the alloy sample for use as a reference. Our measurements are such that the magnetic impurity contribution to the magnetization is obtained by subtracting directly the signal of a pure host sample from the signal of the alloy sample by means of an astatic coil which couples the resultant magnetic flux to a superconducting quantum interference device (SQUID) magnetometer. Figure 1 shows this setup. The magnetization of the sample is measured in a field of 88 Oe trapped in a Nb cylinder surrounding the composite sample, of host reference sample-alloy sample.

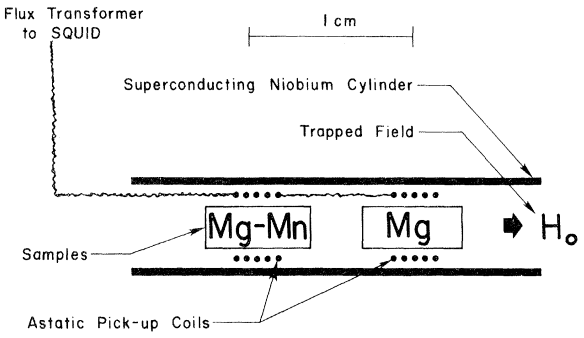

FIG. 1. Details of the magnetometer and samples.

Measurements of the magnetization were taken with the samples inside the mixing chamber (in the dilute phase) of a ^{3}He-^{4}He dilution refrigerator, the temperature being measured with a powder cerium magnesium nitrate thermometer (length equal to diameter) whose magnetization was also monitored with a SQUID magnetometer. With the samples inside the mixing chamber good contact was maintained with the thermometer and at the same time mechanical strains on the soft single crystal samples were minimal. The samples were first cooled in the trapped field to the lowest temperature of ~ 8 mK and then they were warmed up in small increments up to 2 K. The magnetization reading was taken when the sample was in equilibrium with the thermometer; it took about 1 to 2 h to reach equilibrium for each point at the lowest temperatures, equilibrium being established by the circulating ^{3}He.

The SQUID magnetometer was calibrated against the nuclear magnetization of an aluminum sample.[8] Temperature-dependent background contributions from the magnetometer were determined and subtracted by reversing the position of the alloy and the reference sample in a separate experiment. This procedure was necessary for the most dilute samples.

III. RESULTS AND ANALYSIS

A. MgMn single crystal

Figure 1 shows the magnetization per parts per million of impurity along both the c and a axes of a 5-ppm single crystal of *Mg*Mn plotted as a function of

$1/T$. At high temperatures ($T > 1$ K) the magnetization in a field H_0 obeys a Curie-Weiss law of the form

$$M = \frac{CNg^2\mu_B^2 S(S+1)H_0}{3k_B(T+T_c)} \quad (1)$$

with a small Curie-Weiss temperature T_c of ~ 9 mK for the a axis and ~ 15 mK for the c axis, while at low temperatures the magnetization is anisotropic with the a-axis magnetization being larger than the c-axis magnetization. Assuming $g = 2$ and using the experimental value for the high-temperature Curie constant, the effective spin for the Mn ion is $S = 2.3 \pm 10\%$, which is only slightly smaller than the free-ion value of $S = \frac{5}{2}$. Since the Mn impurity is an S-state ion ($L = 0$), the anisotropy in the low-temperature magnetization is assumed to a rise from the combined effects of the crystal field and spin-orbit coupling to excited L-S terms. Under these conditions, the Mn ion can be described by a spin Hamiltonian which, for a crystal field of axial symmetry and an external magnetic field H_0, has the form

$$\mathcal{H} = \mu_B H_0(g_{\parallel}\cos\theta S_z + g_{\perp}\sin\theta S_x) + D[S_z^2 - \tfrac{1}{3}S(S+1)] \ , \quad (2)$$

where θ is the angle between H_0 and the c (or Z) axis. The first term represents an anisotropic Zeeman interaction, while the second term describes the fine-structure splitting of the spin multiplet up to second order in λ, the spin-orbit coupling constant. The parameter D is proportional to λ^2 and is a measure of the size of the fine-structure splitting. If the eigenvalues E_i and eigenvectors $|i\rangle$ of the spin Hamiltonian are known, then the magnetization as a function of temperature can be calculated from the expression:

$$\frac{M}{C} = Ng\mu_B \frac{\sum_i \langle|\vec{S}\cdot\vec{H}_0|\rangle \exp(-E_i/k_BT)}{\sum_i \exp(-E_i/k_BT)} \ . \quad (3)$$

The solid curves in Fig. 2 represent the calculated c-axis and a-axis magnetizations for an impurity with $g = 2$ and $S = \frac{5}{2}$, and with a fine-structure parameter of $D = +0.006$ K. The latter value giving the best fit to the experimental data. The criterion for determining the best-fit value of D was that the corresponding calculated curve provide a good fit to the experimental data over the widest temperature range, starting with the Curie-Weiss region, and that subsequent departures at lower temperatures were such that M(calculated) $-$ M(measured) > 0. Figure 2 shows that, while the agreement between theory and experiment is good at high temperatures, the theoretical curves consistently lie above the measured data at low temperatures. This behavior can be attributed to the presence of impurity-impurity (RKKY) interactions which tend to depress the magnetization below the single-impurity value and reduce the anisotropy between the a and c axes. Based on the sign of the anisotropy ($D > 0$), coupled with the form of the fine-structure splitting (DS_z^2), the energy level diagram shown in Fig. 3 can be proposed for Mn dissolved in Mg and for H_0 parallel to the c axis. The ground state is thus the $\pm\frac{1}{2}$ doublet and the overall

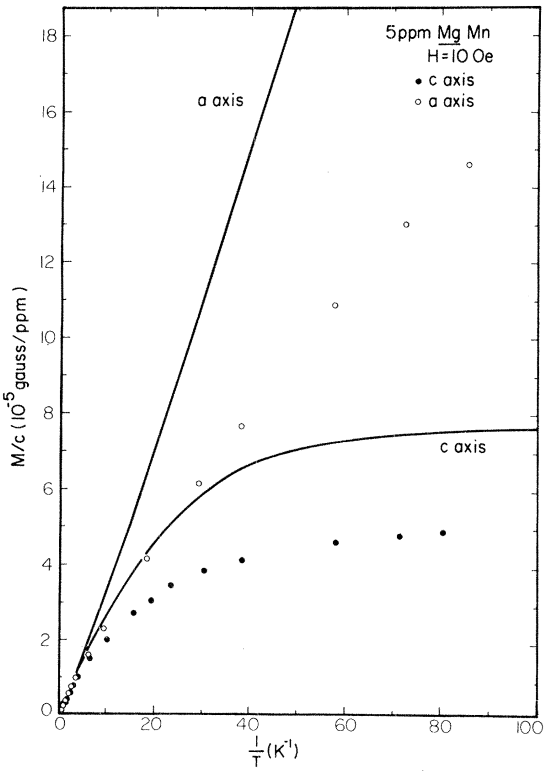

FIG. 2. Magnetization per impurity for Mg-Mn single crystals along the c and a axes.

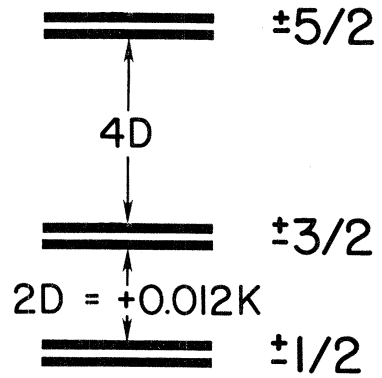

FIG. 3. Energy levels for Mn in Mg which fit out magnetization data on single crystals.

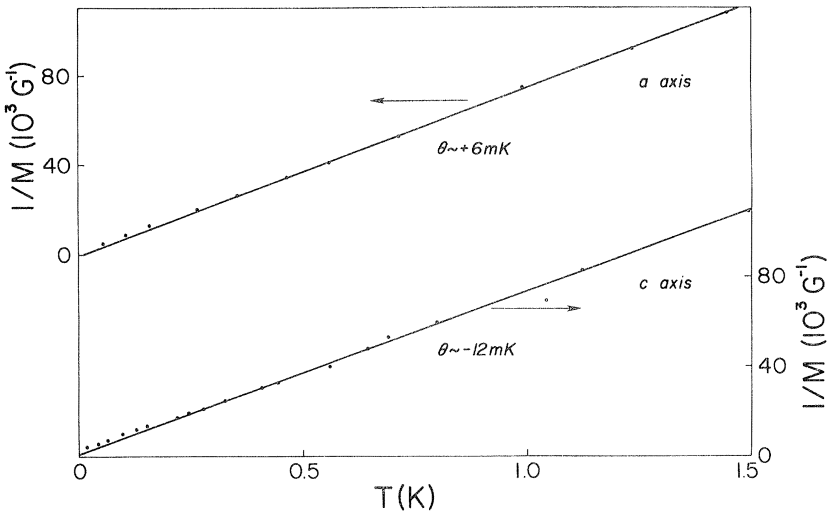

FIG. 4. Curie-Weiss behavior of Mg-Mn along the c and a axes.

splitting due to fine structure is *36* mK. It is interesting that such a fit is consistent with our high-temperature data (0.5 to 2 K), Fig. 4, in that the Curie-Weiss temperature for the a axis is positive while for the c axis it is negative. This is predicted from the high-temperature expression for the magnetization along each direction[9]

$$M_{\parallel} \approx M_0\left(1-\frac{D(2S-1)(2S+3)}{15kT}\right), \qquad M_{\perp} \approx M_0\left(1+\frac{D(2S-1)(2S+3)}{30kT}\right). \tag{4}$$

M_0 being the magnetization in the Curie-law regime (without any interactions). Although the Curie-Weiss temperature "has only limited theoretical significance,"[10] it can provide an indication of the low-temperature behavior from the high-temperature region. It is consistent with our low-temperature interpretation.

B. ZnMn single crystal

Figure 5 shows the magnetization per parts per million of impurity along the c and a axes of two single crystals of *Zn*Mn plotted as a function of $1/T$. As in MgMn, the measured magnetization obeys a Curie-Weiss law at high temperatures, with Curie-Weiss temperatures T_c of less than 30 mK for both samples; the magnetization shows a large anisotropy at low temperatures. However, the sign of the anisotropy in *Zn*Mn is opposite to that in *Mg*Mn, with the measured magnetization along the c axis being larger than that along the a axis. Moreover the measured value of the high-temperature Curie constant yields an effective spin for Mn in Zn of $S=1$ (assuming $g=2$). The large reduction in the effective spin from its free-ion value of $S=\frac{5}{2}$ suggests the possibility of substantial mixing between the d states of the impurity and the free-electron states of the host's conduction band. The *Zn*Mn data were analyzed using the spin Hamiltonian in Eq. (2) and the solid curves in Fig. 5 represent the calculated magnetization for an impurity with $g=2$ and $S=1$, and with a negative fine-structure parameter of $D=-0.070$ K giving the "best fit" to the experimental data. The corresponding energy level scheme for Mn in Zn and for H_0 parallel to the c axis is shown in Fig. 6 and consists of a ± 1 doublet ground-state energy level with a singlet 0-spin state lying above it by 0.070 K.

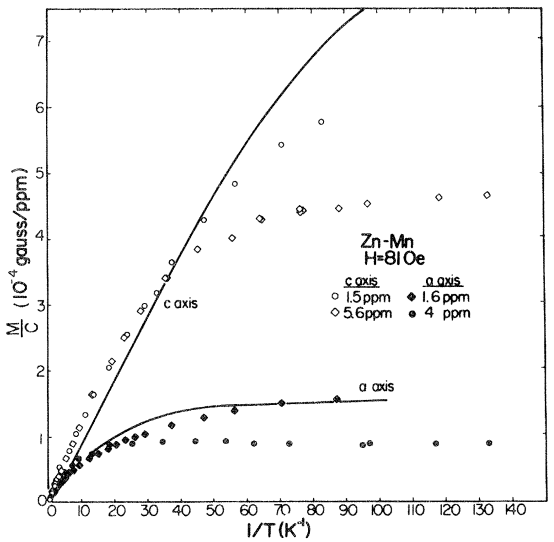

FIG. 5. Magnetization per impurity of Zn-Mn single crystals along the c and a axes.

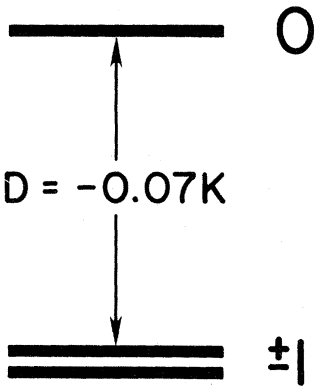

FIG. 6. Energy levels for Mn in Zn which fit our magnetization data on single crystals.

C. Zn-Mn polycrystalline

Figure 7 shows the behavior of the magnetization parts per million of impurity as a function of $1/T$ for a series of polycrystalline *Zn*Mn samples of varying concentration. In order to obtain a precise determination of the effective moment per Mn impurity, three independent methods[6] were used to measure the concentration of Mn impurities in the samples: chemical analysis, resistivity ratios, and neutron activation. The values thus obtained for the impurity concentrations, in combination with the measured values from the high-temperature Curie constants, yield an effective spin of $S=1$ (assuming $g=2$) for all the samples measured, in agreement with the value obtained from the analysis of the single crystal *Zn*Mn data in Fig. 5. The solid curves in Fig. 7 represent theoretical calculations of the magnetization. The curve for $D=0$ shows the behavior of a system of free impurity spins with $S=1$ (Brillouin function), while the curve for $D=-0.070$ K shows the effect of the crystal field on the magnetization (suitably averaged over all possible orientations of the crystallites) using the value of the fine-structure parameter obtained from the analysis of the single crystal data. The data in Fig. 7 further serve to emphasize the importance of impurity-impurity interactions in these systems. Even at the parts per million level, the effect of RKKY interactions is to cause the magnetization per parts per million of impurity to decrease with increasing impurity concentration; hence, the 1-ppm sample represents only an approach toward single-impurity behavior.

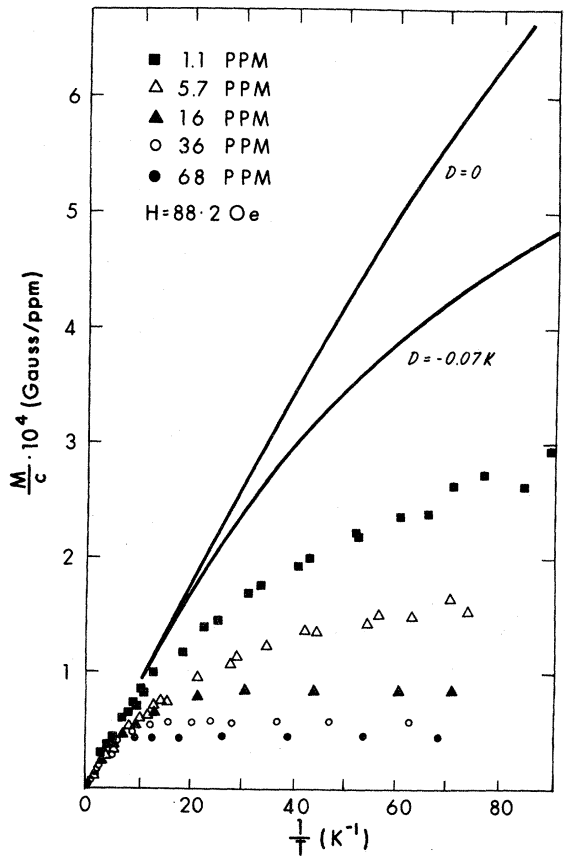

FIG. 7. Magnetization of Zn-Mn polycrystalline samples as a function of $1/T$. The top solid curve is the Brillouin function for a spin of 1 and a field of 88 Oe; lower solid curve is with D.

D. ZnCr single crystal

Figure 8 shows the magnetization per parts per million of impurity along the c and a axis of two single crystals of *Zn*Cr plotted as a function of $1/T$. The

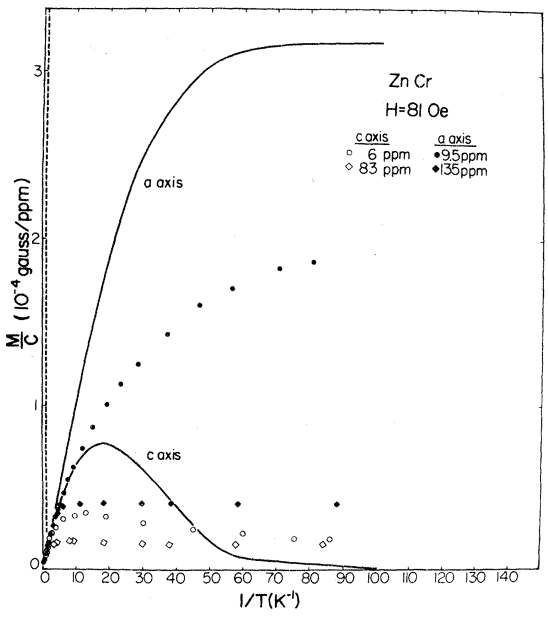

FIG. 8. Magnetization per impurity of Zn-Cr single crystals along the c and a axes.

free-ion configuration of Cr^{2+} corresponds to the Hund's rule term $L=2$, $S=2$. However, ESR measurements[11] on related systems such as *Cu*Cr suggest that the orbital angular momentum of the Cr impurity is quenched by the crystal field of the host. Assuming $g=2$, then the high-temperature Curie-Weiss behavior once again yields an effective spin of $S=1$ (as in *Zn*Mn) and Curie-Weiss temperatures T_c of less than 40 mK. This value of S implies that in the *Zn*Cr system, as well, there is substantial mixing of the impurity's $3d$ states with the conduction band states of the host. At low temperatures, the magnetization in Fig. 8 is anisotropic. However, the sign of the anisotropy is opposite to that for Mn in the same host (Zn), with the a-axis magnetization being larger than the c-axis magnetization. The effect of RKKY interactions is also readily apparent in this system from the reduction of the measured magnetization with increasing impurity concentration. The spin Hamiltonin in Eq. (2) also provides a valid description for systems in which the orbital angular momentum of the impurity has been quenched by crystal fields, and the solid curves in Fig. 8 show the calculated magnetization for an impurity with $g=2$, $S=1$, and a fine-structure parameter of $D=+0.080$ K. The energy level diagram for Cr in Zn is shown in Fig.9 and consists of a singlet 0-spin ground state with the ± 1 doublet lying 80 mK above it.

An interesting feature of the magnetization data in Fig. 8 which lends support to the assignment of an effective spin of $S=1$ to the Cr impurity is the presence of a maximum in the measured c-axis magnetization of both *Zn*Cr single crystals, which becomes more pronounced with decreasing concentration. Such a maximum is present in the calculated c-axis magnetization only for integer spins S and for $D>0$. Moreover, the tendency of the measured c-axis magnetization towards zero at low temperatures reflects the approach toward a nonmagnetic singlet ground state such as that predicted by the energy level diagram in Fig. 9.

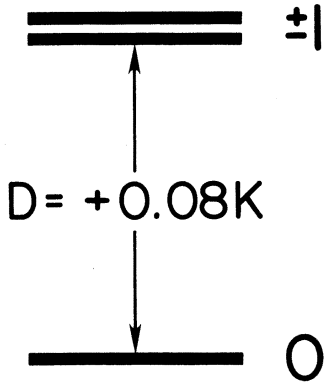

FIG. 9. Energy levels for Cr in Zn which fit our magnetization data on single crystals.

IV. DISCUSSION

Our results for the single crystal alloys show a large anisotropy in the magnetization and we attribute this to fine-structure splitting caused by spin-orbit coupling taken to second order. Since the anisotropy decreases as the RKKY interaction is increased (by increasing the impurity concentration), the anisotropy cannot be attributed to the RKKY interaction as suggested by Dixon and Dupree.[12] This is substantiated by a fit to our data on Mg-Mn which uses an isotropic RKKY interaction.[13] In spite of the fact that our most dilute samples with a few parts per million of magnetic impurity show strong effects of RKKY interactions, the ground state for each impurity can be readily identified in our temperature range. It is interesting that a simple ionic model can explain our results for systems such as Mg-Mn as well as Zn-Mn and Zn-Cr where the mixing between impurity states and conduction electron states is strong as evidenced by a reduction of the spin from $S=\frac{5}{2}$ to $S=1$ (for Zn-Mn and Zn-Cr). We are aware that our analysis is by no means complete and if the effective spin were non-half-integer, then we would have no model for making the simple calculations that we present here.

One of the most interesting aspects of the results is the change of sign of the fine-structure splitting depending on the impurity and the host. Riseborough[14] has proposed an explanation for the change of sign in the fine-structure constant in going from Zn-Mn to Zn-Cr. His calculation is in excellent agreement with our data and is based on treating the magnetic impurity within the Anderson model by including the spin-orbit coupling.

The fit to calculated curves, as mentioned earlier, is not in exact agreement. This is due to the presence of RKKY interactions, even in the most dilute samples. Correction for impurity-impurity interactions should give much better agreement; this will be discussed in a forthcoming publication.[15]

Another interesting feature of our data is that there is no evidence for a Kondo spin-compensated state in our temperature range. All previous measurements at high temperatures claimed $T_K \sim 0.90$ K to 0.25 K. We do not see it in our high-temperature Curie-Weiss temperatures which are very small (40 mK and less) nor in the low-temperature data which show only fine-structure behavior with some RKKY interactions. The concentration of impurities is so low that the Kondo state should have been observed especially in the temperature region where it was claimed to be. Our data extend to such low temperatures that the ground state of the system is clear: inspite of the fact that some RKKY interactions still remain, the ground state for each impurity can be readily identified as shown in the energy levels diagrams. Resistivity data of Kastner and Wassermann[7]

suggest that perhaps the estimates of the Kondo temperatures were too high due to impurity-impurity interactions.

Since hyperfine interactions can also contribute to single impurity behavior in the alloys studied here, and in particular the Mn alloys, a computation was made of the magnetization in that case. Using values of hyperfine fields obtained in nuclear orientation studies, the effect on the magnetization is small in our measurements. However the hyperfine interaction will be of importance in the millikelvin region.

Comparison of our data with other groups who have worked at high temperatures shows some agreement. The signs of our fine-structure splitting agree with the susceptibility and measurements of Refs. 1 and 16. The magnitude of the fine-structure constant for Mg-Mn is in agreement with resonance data of Oseroff and Suhl.[17]

The energy-level diagrams in Figs. 3, 6, and 9 have important consequences for the electrical resistivity. An essential feature of the Kondo model for the scattering of conduction electrons from a magnetic impurity is the presence of second-order spin-flip scattering processes in which the z component of the impurity spin in the intermediate state differs by ± 1 from its value in either the initial or the final state. When the S_z states of the impurity are degenerate, the localized spin can flip without energy expenditure and this leads to a strong resonance at $T=0$ in the transition probability for the scattering of conduction electrons having energies $E_k = E_F$. However, if the degeneracy of the impurity levels is partially lifted by the crystal field, then Maranzana[18] has shown that pairs of nondegenerate S_z eigenstates differing by ± 1 lead to additional resonances at $T=0$ in the conduction electron transition probability shifted away from the Fermi energy and having energies E_k to the energy separation of the pair of levels. Such resonances at $E_k \neq E_F$ appear as peaks in the resistivity-temperature curve occurring at temperatures which roughly correspond to the distances between pairs of resonating levels. The energy scheme for MgMn in Fig. 3 implies that the resistivity will possess 2 peaks, one at $2D$ corrresponding to the pair of doublets $|\pm 1/2\rangle$ $|\pm 3/2\rangle$ and one at $4D$ corresponding to the pair $|\pm 3/2\rangle|\pm 5/2\rangle$. Moreover, since the $|\pm 1/2\rangle$ doublet is the lowest level, the resistivity will also show the normal Kondo resonance and subsequent spin compensation as $T \rightarrow 0$. For ZnMn and ZnCr, and inspection of the energy level diagrams in Figs. 6 and 9 shows that the resistivity-temperature curve for these two systems will possess only one peak at $T \sim D$ corresponding to the resonant pair $|0\rangle|\pm 1\rangle$. Since the ground state of these two systems ($|0\rangle$ for ZnCr and $|\pm 1\rangle$ for ZnMn) will not support spin-flip scattering, neither system will exhibit the normal Kondo resonance.

Our analysis invoked an ionic[19] model in treating the magnetic impurity in a metallic host. However the metallic state brings in a great deal of mixing between the conduction electron states and the $3d$ states as evidenced by the greatly reduced effective spin. Nonetheless, once this reduced effective spin is obtained, there seems to be some validity in using ionic types of calculations with fine-structure splitting to calculate the behavior of the impurity.

ACKNOWLEDGMENTS

We wish to thank Dr. S. Kral and T. Steelhammer for their help in the early stages of this work. We thank Professor R. Orbach and Professor W. Weyhmann for many stimulating discussions. All our samples were made by the Crystal Growth Group of the Physics Dept., University of Utah. This research was supported by the National Science Foundation. One of us (R.R.) would like to thank the National Research Council of Canada for a postdoctoral Fellowship.

---

*Present address: National Semiconductor, Santa Clara, Calif. 95051.

[1]P. L. Li, F. T. Hedgcock, W. N. Muir, and J. O. Strom-Olsen, Phys. Rev. Lett. 31, 29 (1973).
[2]A. E. Bell and A. D. Caplin, J. Phys. F 5, 143 (1975).
[3]R. Harris, F. T. Hedgcock, J. O. Strom-Olsen, and M. J. Zuckermann, Can. J. Phys. 52, 1765 (1974).
[4]R. S. Newrock, B. Serin, J. Vig, and G. Boats, J. Low Temp. Phys. 5, 701 (1971).
[5]F. W. Smith, Phys. Rev. B 10, 2980 (1974).
[6]J. C. Doran, S. F. Kral, T. Steelhammer, and O. G. Symko, Solid State Commun. 17, 1099 (1975).
[7]J. Kastner and E. F. Wassermann, J. Low Temp. Phys. 29, 411 (1977).
[8]T. J. Steelhammer and O. G. Symko, Rev. Sci. Instrum. 50, 532 (1979).
[9]R. Hudson, *Principles and Application of Magnetic Cooling* (North-Holland, Amsterdam, 19772).
[10]P. W. Selwood, *Chemisorption and Magnetization* (Academic, New York, 1975).
[11]P. Monod and S. Schultz, Phys. Rev. 173, 645 (1968).
[12]J. M. Dixon and R. Dupree, Solid State Commun. 16, 1301 (1975).
[13]P. Gash, R. Roshko, and O. G. Symko, J. Appl. Phys. 52, 1720 (1981).
[14]P. S. Riseborough, Phys. Rev. B 20, 1362 (1979).
[15]P. Gash, R. Roshko, and O. G. Symko (unpublished).
[16]J. L. Benchimol, F. T. Hedgcock, and J. O. Strom-Olsen, in *Crystal Field Effects in Metals and Alloys,* edited by A. Furrer (Plenum, New York, 1976), p. 158.
[17]S. Oseroff, B. Gehman, and S. Schultz, Phys. Rev. B 15, 1291 (1977).
[18]F. E. Maranzana, Phys. Rev. Lett. 25, 239 (1970).
[19]L. L. Hirst, Z. Phys. 241, 9 (1971).